Designing Radio Interferometric Positioning Systems for Indoor Localizations in Millimeter Wave Bands

Marie Shinotsuka*, Yiyin Wang†, Xiaoli Ma*, and G. Tong Zhou*
*School of Electrical and Computer Engineering, Georgia Institute of Technology, Atlanta, Georgia 30332–0250
†Department of Automation, Shanghai Jiao Tong University, Shanghai, 200240, China

***Abstract*—Recently, millimeter wave (MMW) systems that operate at 60 GHz are proposed for the short-range communications to reduce the interference. Taking advantage of the spectrum characteristics of MMW bands, the indoor localization system using the radio interferometric positioning system (RIPS) employing space-time coding is proposed in this paper. The RIPS is a promising localization scheme for its low complexity and high accuracy, and the space-time RIPS (STRIPS) is the enhancement of the RIPS to work in MMW bands under the flat-fading channel. Two anchor nodes simultaneously transmit at two time slots with different frequencies, and the signal is sampled at the low-sampling frequency at the target node. The STRIPS achieve the range-difference (RD) estimate without approximation and is immune to channel fading effects. To accommodate the frequency offsets, the ESPRIT-based algorithm is adopted. Monte-Carlo simulation results are presented to confirm the performance of the STRIPS.**

***Keywords*—Radio interferometric positioning system (RIPS), localization, time-difference-of-arrival (TDOA), range-difference (RD), synchronization.**

I. Introduction

For its wide applications such as product tracking in the warehouse, failure detections of the buildings and location detection of personnels, indoor localizations have attracted attentions from industry and academia [1]. However, indoor environments are likely to have multipath reflections, which cause the channel fading, and most indoor applications require submeter accuracy. Moreover, interferences among users in the spectrum are causing problems not only to the indoor localization systems but also to the wireless communication systems in general.

Millimeter wave (MMW) communication systems, which operates in 60 GHz band, are recently proposed as a solution to this interference problem and alleviate the traffic in the spectrum of 300 MHz -3 GHz range [2]–[4]. In the past, this 60 GHz band was considered to be inadequate for wireless communications due to its high signal attenuation property. Recently, however, this property has been reconsidered as an advantage for short-range communication systems since it allows high frequency reuse in the limited area and is less likely to cause interference [2]. Furthermore, the coherent bandwidth of the channel is in the order of MHz as the multipath components in MMW bands are limited [4]. These characteristics also benefit the indoor localization systems, and the short communication range of MMW signals suffices their purpose.

MMW-based indoor localization systems are already proposed in [5]–[8]. The power attenuation of the received signal strength (RSS) is used to estimate the distance in [5], where the RSS is measured over different distances ranging up to one meter using various materials as the base, and the attenuation patterns of the MMW signals are observed. Using the material that produces the most smooth RSS decay with increase in the distance, the average accuracy of 3 cm is achieved in the experiment. Another approach is to use the 60 GHz OFDM signal, where the differential time-difference-of-arrival (DTDOA) [6] and round-trip time (RTP) [7] are estimated to accommodate clock offsets, and the experiment achieved the accuracy in the range of 10-30 cm. In [8], the impulses of MMWs are employed to estimate the time-difference-of-arrival (TDOA), and their experiment in a regular classroom achieves the accuracy of 15-40 cm. Although these MMW-based indoor localization systems have shown to achieve high accuracy, most of these systems only consider the additive white Gaussian noise (AWGN) channels or assume that the knowledge of the channel is already available. Furthermore, they require high sampling rate. To meet these challenges, we introduce the radio interferometric positioning system (RIPS) for indoor localizations in MMW bands.

The RIPS [9] is the time-based localization algorithm originally proposed for wireless-sensor networks (WSNs) that achieves high accuracy at low complexity. The basic idea behind the RIPS is to observe the phase of a low-frequency differential signal component created by two sinusoids at slightly different frequencies. Outdoor experiments presented in [9] achieved the average accuracy of 2 cm. For its simplicity and high performance, various groups have improved the RIPS and applied to different scenarios. The RIPS in the 2.4 GHz range using the natural instability in oscillators to create the frequency difference between transmitters is presented in [10], [11], and obtains the accuracy of few meters in their experiments. The RIPS is also extended to mobile nodes by taking the Doppler shifts into account [12]. Moreover, the spinning beacons are used to produce Doppler signals in [13] and achieve the angle-of-arrival (AOA) estimates. The RIPS employing the linear chirp signals is proposed in [14], [15] to solve the integer ambiguity issue and to deal with clock offsets. In [16], transmitters employ frequency hopping and transmit at multiple frequencies to sound the channels and

Y. Wang was supported by the NSF of China (No. 61301223) and the NSF of Shanghai (No. 13ZR1421800).

accommodate the multipath environment. Furthermore, the asynchronous RIPS (ARIPS) is proposed to make use of dual-tone signaling to obtain TDOA estimates, and it is robust to the carrier frequency offsets (CFOs) among transmitters. Most RIPS systems proposed so far have only considered the AWGN channels, and their range estimators have approximations, whose size depends on the chosen parameters. Moreoever, the resolvable range is limited by the size of carrier frequencies due to the phase wrapping. Therefore, we propose the RIPS for MMW bands that is robust to the channel fading by employing the space-time coding.

In this paper, the space-time radio interferometric positioning system (STRIPS) is developed. Three nodes participate at each ranging session, where two anchor nodes (nodes with known positions) transmit at different frequencies at two time slots. At the receiver, the range difference (RD) is estimated. By designing transmitting frequencies to be within the coherent bandwidth of the channel, the STRIPS can effectively work with the flat-fading channel. At the receiver, the range information is extracted from the low-frequency differential signal by squaring the received signal. Time synchronization among two anchor transmitters is required, but no synchronization requirements are imposed between anchor nodes and the target receiver, which allows new target nodes to freely enter the network. The ESPRIT-based frequency estimation algorithms are proposed to estimate the transmitted frequencies from the sampled signal to accommodate frequency offsets between transmitters. The RD estimate is free of approximation errors unlike the range estimates of the exiting RIPS's [9], [17], and the localization can be performed using the available RD-based localization algorithms [18] [19]. The acquisition range without the integer ambiguity is determined by the frequency difference and independent of the size of the carrier frequency. Therefore, we can obtain the necessary acquisition range adequate for indoor scenarios despite of high carrier frequencies.

In summary, our proposed STRIPS has several advantages: 1) the receiver is only required to sample at a low-sampling rate; 2) the receiver is robust to flat-fading channels; 3) the RD estimator has no approximation errors; 4) the resolvable range without the integer ambiguity is independent of the size of the carrier frequency; 5) frequency offsets in anchor nodes are accommodated; and 6) no time or frequency synchronization requirement is imposed on the target node.

The rest of the paper is organized as follows. The transmitter system model of the STRIPS is introduced in Section II. The ranging in the STRIPS as well as the ESPRIT-based frequency estimation algorithm are presented in Section III. The simulation results are presented in Section IV, and the paper concludes in Section V.

II. The System Model

A radio interferometric positioning system employing two transmitters and a receiver is illustrated in Fig. 1. Two anchor nodes transmit sinusoids at different frequencies, and the target node receives a sum of two transmitted sinusoids. In the STRIPS, anchor nodes transmit sinusoids at two time slots

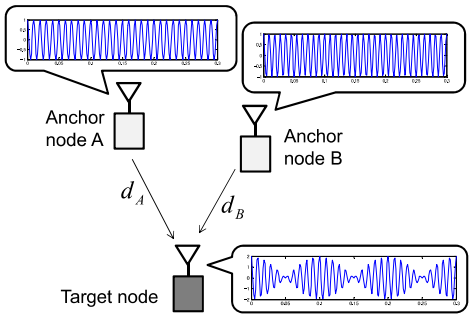

Fig. 1. Radio interferometric ranging technique.

with different frequencies. At the first time slot, nodes A and B transmit at frequencies f_c and f_c+f_d, respectively, where f_c is the carrier frequency, f_d is the frequency difference between signals transmitted by two nodes, and $f_c \gg f_d$. At the second time slot, node A transmits at $f_c - f_d$, and node B transmits at f_c. For brevity, let us denote designed transmitting frequencies at the mth anchor node at the ith time slot as $f_{m,i}$; hence, at the first time slot, $f_{A,1} = f_c + f_d$ and $f_{B,1} = f_c$. The sequence of transmitted frequencies is summarized in Table I.

	node A	node B
time slot 1	$f_c + f_d$	f_c
time slot 2	f_c	$f_c - f_d$

TABLE I. Transmitted Frequencies at Two Time Slots

Using the bandpass complex representation, the transmitted signals at the first time slot from the mth anchor node can be expressed as

$$s_{m,1}(t) = a_m e^{j2\pi(f_{m,i}+\epsilon_m)(t-t_0)}, \tag{1}$$

where a_m is the complex amplitude of the signal transmitted by the mth node, ϵ_m is the frequency offset at the mth node due to the unreliability of the oscillator, and t_0 is the unknown time instant that anchor nodes start their transmissions. Here, anchor nodes are assumed to be perfectly synchronized in time. At the second time slot, the mth anchor node transmits the signal given as

$$s_{m,2}(t) = a_m e^{j2\pi(f_{m,2}+\epsilon_m)(t-t_0-T_0)}, \tag{2}$$

where T_0 is the time interval between two transmissions. We assume that the frequency offsets at each node are constant over the ranging session.

In the STRIPS, the frequencies are designed so that f_d to be smaller than the coherent bandwidth of the channel. Hence, two signals at different frequencies transmitted by a given anchor node at two time slots experience the same fading channel [20]. Furthermore, we need to keep the time required to complete one ranging session to be within the coherence time of the channel in order to assume that the fading channel experienced by signals is constant over two time slots. Denoting the signal length of $s_{m,i}(t)$ as T_s, the total

time required to complete one ranging session is $T_r = T_s + T_0$. Thus, we design T_s and T_0 to achieve $T_r < T_c$, where T_c is the channel coherence time.

Fig. 2 illustrates the system model under the flat-fading channel. Transmitted signals go through the flat-fading channel and are delayed by a respective propagation delay. The received signal at the target node is the sum of those two faded signals plus the additive white Gaussian noise (AWGN).

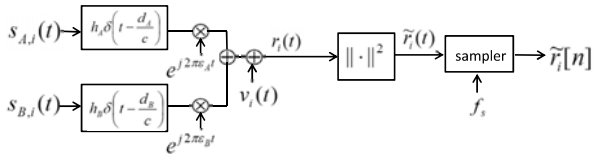

Fig. 2. An illustration of the system model.

Hence, the received signals at two time slots are expressed as

$$\begin{aligned} r_1(t) &= h_A a_A e^{j2\pi(f_{A,1}+\epsilon_A)(t-t_0-\frac{d_A}{c})} \\ &+ h_B a_B e^{j2\pi(f_{B,1}+\epsilon_B)(t-t_0-\frac{d_B}{c})} + v_1(t), \quad (3) \\ r_2(t) &= h_A a_A e^{j2\pi(f_{A,2}+\epsilon_A)(t-t_0-\frac{d_A}{c}-T_0)} \\ &+ h_B a_B e^{j2\pi(f_{B,1}+\epsilon_B)(t-t_0-\frac{d_B}{c}-T_0)} + v_2(t), \quad (4) \end{aligned}$$

where d_m is the distance between the mth anchor node and the target node, c is the speed of light, h_m is the complex-valued channel coefficient of the channel between the mth node and the target node, and $v_i(t)$ is the AWGN at the ith transmission with zero mean and variance σ_n^2.

III. The Receiver Design

A. Range Estimation

At the receiver, the received signal is squared by multiplying $r_i(t)$ with its complex conjugate to obtain the low-frequency differential signal as illustrated in Fig. 2. At the first time slot, the squared signal is given as

$$\begin{aligned} &r_1(t)r_1^*(t) = \|h_A\|^2\|a_A\|^2 + \|h_B\|^2\|a_B\|^2 \\ &+ h_A h_B^* a_A a_B^* e^{j2\pi(f_{A,1}+\epsilon_A)(t-t_0-\frac{d_A}{c})} e^{-j2\pi(f_{B,1}+\epsilon_B)(t-t_0-\frac{d_B}{c})} \\ &+ h_A^* h_B a_A^* a_B e^{-j2\pi(f_{A,1}+\epsilon_A)(t-t_0-\frac{d_A}{c})} e^{j2\pi(f_{B,1}+\epsilon_B)(t-t_0-\frac{d_B}{c})} \\ &+ \tilde{v}_1(t), \end{aligned} \quad (5)$$

where $(\cdot)^*$ denotes conjugate, and $\tilde{v}_1(t)$ includes all the cross terms with $v_1(t)$. The first two terms in (5) are DC terms. Removing these DC terms from (5), the low-frequency differential signal is obtained as

$$\begin{aligned} \tilde{r}_1(t) &= \alpha e^{j2\pi(f_d+\epsilon)t} e^{-j2\pi f_d \frac{d_A}{c}} \\ &+ \alpha^* e^{-j2\pi(f_d+\epsilon)t} e^{j2\pi f_d \frac{d_A}{c}} + \tilde{v}_1(t), \end{aligned} \quad (6)$$

where $\epsilon = \epsilon_A - \epsilon_B$ and $\alpha = h_A h_B^* a_A a_B^* e^{-j2\pi f_c \frac{d_{AB}}{c}} e^{-j2\pi(\epsilon_A(t_0+\frac{d_A}{c})-\epsilon_B(t_0+\frac{d_B}{c}))} e^{-j2\pi f_d t_0}$ with $d_{AB} = d_A - d_B$, which is the RD that we want to estimate. Likewise, at the second time slot, we obtain

$$\begin{aligned} \tilde{r}_2(t) &= \alpha e^{j2\pi(f_d+\epsilon)t} e^{-j2\pi f_d \frac{d_B}{c}} e^{-j2\pi(f_d+\epsilon)T_0} \\ &+ \alpha^* e^{-j2\pi(f_d+\epsilon)t} e^{j2\pi f_d \frac{d_B}{c}} e^{j2\pi(f_d+\epsilon)T_0} + \tilde{v}_2(t), \end{aligned} \quad (7)$$

where $\tilde{v}_2(t)$ contains all the cross terms multiplied with $v_2(t)$. Notice that α is the unknown complex value that is contant over two time slots.

After squaring $r_i(t)$, both (6) and (7) only have low frequency components at $\pm(f_d + \epsilon)$. Sampling both $\tilde{r}_1(t)$ and $\tilde{r}_2(t)$ at the rate $f_s > 2f_d$ and collecting N samples at each time slot, the column vector $\tilde{\mathbf{r}}$ is formed as

$$\tilde{\mathbf{r}} = \mathbf{S}\mathbf{x} + \tilde{\mathbf{v}}, \quad (8)$$

where $\tilde{\mathbf{r}} = [\tilde{\mathbf{r}}_1^T \ \tilde{\mathbf{r}}_2^T]^T$ with $\tilde{\mathbf{r}}_i$ and $\tilde{\mathbf{v}}$ denote sampled vectors of $\tilde{r}_i(t)$ and $\tilde{v}_i(t)$, respectively, $\mathbf{x} = [\theta_A, \ \theta_A^*, \ \theta_B, \ \theta_B^*]^T$ with $\theta_A = \alpha e^{-j2\pi f_d \frac{d_A}{c}}$ and $\theta_B = \alpha e^{-j2\pi f_d \frac{d_B}{c}} e^{-j2\pi(f_d+\epsilon)T_0}$, and

$$\mathbf{S} = \begin{bmatrix} \mathbf{S}_0 & \mathbf{0}_{N\times 2} \\ \mathbf{0}_{N\times 2} & \mathbf{S}_0 \end{bmatrix}, \quad (9)$$

with $\mathbf{S}_0 = [\mathbf{s}_N(f_d+\epsilon, f_s) \ \mathbf{s}_N^*(f_d+\epsilon, f_s)]$ and $\mathbf{s}_N(f, f_s) = [1, e^{j2\pi f/f_s}, \ ..., \ e^{j2\pi f(N-1)/f_s}]^T$.

Representing the ith element of $\mathbf{x}$ as $[\mathbf{x}]_i$, notice that

$$([\mathbf{x}]_1^* + [\mathbf{x}]_2)([\mathbf{x}]_3 + [\mathbf{x}]_4^*) = 4\|\alpha\|^2 e^{-j2\pi(f_d+\epsilon)T_0} e^{j2\pi f_d \frac{d_{AB}}{c}}. \quad (10)$$

Here, T_0 is assumed to be known at the receiver. As seen in (10), the unknown complex term α appears as $\|\alpha\|^2$, which no longer impacts the estimation of the phase.

If the accurate $\mathbf{S}$ is known, $\mathbf{x}$ can be estimated by a least-squares (LS) estimator as

$$\hat{\mathbf{x}} = \mathbf{S}^\dagger \tilde{\mathbf{r}}, \quad (11)$$

where $(\cdot)^\dagger$ denotes the pseudo-inverse. From (10), the RD estimator is given by

$$\hat{d}_{AB} = \frac{c}{2\pi f_d} \angle\{e^{j2\pi(f_d+\epsilon)T_0}([\hat{\mathbf{x}}]_1^* + [\hat{\mathbf{x}}]_2)([\hat{\mathbf{x}}]_3 + [\hat{\mathbf{x}}]_4^*)\}. \quad (12)$$

B. Frequency Estimation

When $\epsilon_A = \epsilon_B$, $\epsilon = 0$ and $\mathbf{S}$ can be accurately calculated. However, in the case where $\epsilon_A \neq \epsilon_B$, the receiver has to estimate the frequency from the sampled signal to construct the accurate $\mathbf{S}$. In this paper, the ESPRIT-based method is employed for frequency estimation since it finds a closed-form solution [21], [22].

For this discussion, let us ignore the noise term for simplicity. A sum of sampled received signals at two time slots $\check{\mathbf{r}} = \tilde{\mathbf{r}}_1 + \tilde{\mathbf{r}}_2$ is modeled as

$$\check{r}[n] = \check{\alpha} e^{j2\pi(f_d+\epsilon)/f_s n} + \check{\alpha}^* e^{-j2\pi(f_d+\epsilon)/f_s n}, \quad (13)$$

where $\check{\alpha} = \alpha(e^{-j2\pi f_d \frac{d_A}{c}} + e^{-j2\pi f_d \frac{d_B}{c}} e^{j2\pi f_d + \epsilon T_0})$. Now, rearrange $\check{\mathbf{r}}$ into a matrix $\mathbf{R}_{(L\times N-L+1)}$ as

$$\mathbf{R} = [[\check{\mathbf{r}}]_{1:L-1}, \ [\check{\mathbf{r}}]_{2:L}, \ ..., \ [\check{\mathbf{r}}]_{N-L:N-1}] \quad (14)$$

where L is a parameter chosen between $N/3$ and $N/2$.

Notice that $\mathbf{R}$ has a shift-invariant property. Hence, we define the following matrices:

$$\mathbf{R}_1 = [\mathbf{I}_{L-1}\ \mathbf{0}_{L-1}]\mathbf{R},\ \mathbf{R}_2 = [\mathbf{0}_{L-1}\ \mathbf{I}_{L-1}]\mathbf{R}. \quad (15)$$

In other words, $\mathbf{R}_1$ and $\mathbf{R}_2$ contain the first and the last $L-1$ rows of $\mathbf{R}$, respectively. It has been shown that the general eigenvalues of the matrix pair $\{\mathbf{R}_1, \mathbf{R}_2\}$ are given by $\lambda_1 = e^{j2\pi(f_d+\epsilon)/f_s}$ and $\lambda_2 = e^{-j2\pi(f_d+\epsilon)/f_s}$. Therefore, obtaining the eigenvalues of $\mathbf{R}_1^{\dagger}\mathbf{R}_2$, we can estimate ϵ by

$$\hat{\epsilon} = \frac{f_s}{2\pi}\angle(\lambda_1 + \lambda_2^*) - f_d. \quad (16)$$

Once we estimate ϵ, we can use it to construct $\mathbf{S}$ and further estimate the RD using the estimator given in (12).

IV. Simulation Results

In this section, the performance of the STRIPS is evaluated and compared with the RIPS [9] through Monte-Carlo simulations. Five anchor nodes placed at corners and the center of the 10×10 meters square and the target node randomly placed within the square at each Monte-Carlo run, and 2000 iterations are performed. For the STRIPS, we choose $f_c = 60$ GHz, $f_d = 10$ MHz, $f_0 = 59.9$ GHz, the signal length of $T_s = 3$ μs, $f_s = 46$ MHz, and $T_0 = T_s$. The resolvable RD without the integer ambiguity is given as $[-\frac{c}{2f_d}, \frac{c}{2f_d}]$; thus, $f_d = 10$ MHz allows the RD estimations up to ± 15 meters without the integer ambiguity. Hence, each ranging session takes 6 μs, which is less than the typical coherence time in MMW bands. The CFO is randomly generated from $[-60\text{ kHz}, 60\text{ kHz}]$.

For the RIPS, we let the carrier frequency to be f_d; therefore, the resolvable range without the integer ambiguity for the RIPS is the same as that of the STRIPS. The frequency difference at two transmitteres is $\delta = 1$kHz, and the same number of samples as the STRIPS is obtained at the rate $4\delta = 4$ kHz. The CFO is randomly generated $[-100\text{ Hz}, 100\text{ Hz}]$. When the Q-range involves three anchor nodes, the Q-range can be converted to the RD between two transmitters and the receiver target node [23]. Hence, we employed the RD-based localization in [18] for both the RIPS and the STRIPS to estimate the position of the target node. The transmitting power at two transmitter nodes is fixed to be 1, and the signal-to-noise ratio (SNR) is defined as $1/\sigma_n^2$.

First, we consider the case where there is only the AWGN and no fading. The root-mean-square error (RMSE) of the location estimates vs. SNR for the STRIPS and the RIPS is shown in Fig. 3. When there is no CFO, the STRIPS and the RIPS achieve similar performance. Despite of the large CFO, the STRIPS effectively accommodates CFOs and can achieve a submeter accuracy at SNR > 15 dB.

Second, let us consider the case with the fading. Since MMW signals have strong attenuation, the existance of line-of-sight (LOS) between the anchors and the target node is assumed. Therefore, the channel is assumed to be Rician distributed, as the measurements in a home and an office environments in the 60 GHz band are shown to have high Rician factor K in the range of $8 \sim 11$ dB [24]. In the simulation, we use $K = 10$ dB, and the channel coefficients

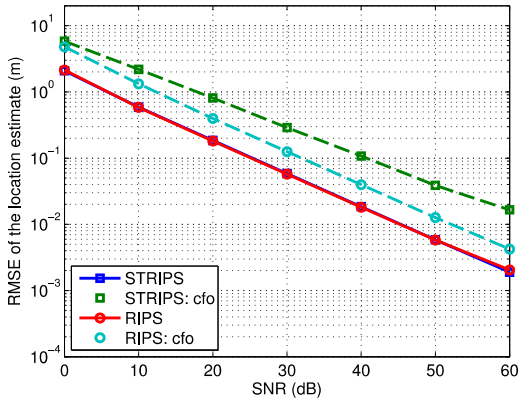

Fig. 3. The RMSE of the location estimate vs. SNR under the AWGN channel.

are randomly generated at each iteration. The RMSE of the location estimates under fading for the RIPS and the STRIPS is shown in Fig. 4. While the RIPS fails to work under the fading scenario, the STRIPS is robust to the fading.

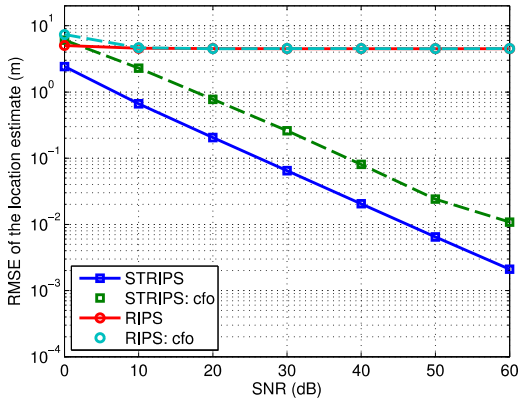

Fig. 4. The RMSE of the location estimate vs. SNR under the flat-fading channel.

V. Conclusions

In this paper, we developed the space-time radio interferometric positioning system (STRIPS) in millimeter wave (MMW) bands for indoor localizations. The STRIPS transmits sinusoids with different frequencies at two time slots, and the range-difference (RD) estimates can be achieved from the phase of the low-frequency differential signal. The frequency estimation method is proposed to accommodate frequency offsets due to unreliable oscillators. Despite of the operation in the extremely high frequencies, the parameters in the

STRIPS can be designed to obtain the resolvable range without the integer ambiguity that covers typical indoor localization scenarios. Monte-Carlo simulations confirm the efficiency of the STRIPS.

REFERENCES

[1] H. Liu, H. Darabi, P. Banerjee, and J. Liu, "Survey of wireless indoor positioning techniques and systems," *IEEE Trans. Syst., Man, Cybern. C*, vol. 37, no. 6, pp. 1067–1080, Nov. 2007.

[2] Terabeam Corporation, "Performance characteristics of 60 GHz communication systems," Oct. 2002. [Online]. Available: http://www.terabeam.com/downloads/whitepaperss/TB_60_Ghz.pdf

[3] P. Smulders, "Exploiting the 60 GHz band for local wireless multimedia access: Prospects and future directions," *IEEE Commun. Mag.*, vol. 40, no. 1, pp. 140–147, Jan. 2002.

[4] Z. Pi and F. Khan, "An introduction to millimeter-wave mobile broadband systems," *IEEE Commun. Mag.*, vol. 49, no. 6, pp. 101–107, Jun. 2011.

[5] H. R. Fang, G. P. Cao, E. A. Gharavol, K. Tom, and K. Mouthaan, "60 GHz short range planar RSS localization," in *Proc. IEEE APMC*, Yokohama, Japan, Dec. 2010, pp. 1396–1399.

[6] F. Winkler, E. Fischer, E. Grab, and G. Fischer, "A 60 GHz OFDM indoor localization system based on DTDOA," in *Proc. IST Mobile and Wireless Communications Summit*, Dresden, Germany, Jun. 2005.

[7] T. Ohlemueller, F. Winkler, and E. Grass, "Radio localization in OFDM networks using the round trip phase," in *Proc. IEEE WPNC*, Dresden,Germany, Mar. 2010, pp. 23–27.

[8] M. Bocquet, C. Loyez, M. Fryziel, and N. Rolland, "Millimeter-wave broadband positioning system for indoor applications," in *Proc. IEEE MTT*, Montreal, QC, Canada, Jun. 2012, pp. 1–3.

[9] M. Maróti, B. Kusý, G. Balogh, P. Völgyesi, A. Nádas, K. Molnár, S. Dóra, and A. Lédeczi, "Radio interferometric geolocation," in *Proc. ACM SenSys*, San Diego, CA, Nov. 2005, pp. 1–12.

[10] B. J. Dil and P. J. M. Havinga, "A feasibility study of RIP using 2.4 GHz 802.15.4 radios," in *Proc. IEEE MASS*, San Francisco, CA, Nov. 2010, pp. 690–696.

[11] ——, "Stochastic radio interferometric positioning in the 2.4 GHz range," in *Proc. ACM SenSys*, Seattle, WA, Nov. 2011, pp. 108–120.

[12] B. Kusy, J. Sallai, G. Balogh, and A. Ledeczi, "Radio interferometric tracking of mobile wireless nodes," in *Proc. ACM MobiSys*, San Juan, Puerto Rico, Jun. 2007, pp. 139–151.

[13] H.-l. Chang, J.-b. Tian, T.-T. Lai, H.-H. Chu, and P. Huang, "Spinning beacons for precise indoor localization," in *Proc. ACM SenSys*, Raleigh, NC, Nov. 2008, pp. 127–140.

[14] W. Zhang, Q. Yin, and W. Wang, "Distributed TDOA estimation for wireless sensor networks," in *Proc. IEEE ICASSP*, Dallas, TX, Mar. 2010, pp. 2862–2865.

[15] ——, "Distributed localization for wireless sensor networks using LFM waves," in *Proc. IEEE WCNC*, Sydney, Australia, Apr. 2010, pp. 1–5.

[16] W. Zhang, Q. Yin, X. Feng, and W. Wang, "Distributed TDoA estimation for wireless sensor networks based on frequency-hopping in multipath environment," in *Proc. IEEE VTC*, Taipei, Taiwan, May 2010, pp. 1–5.

[17] Y. Wang, M. Shinotsuka, X. Ma, and M. Tao, "Design an asynchronous radio interferometric positioning system using dual-tone signaling," in *Proc. IEEE WCNC*, Shanghai, China, Apr. 2013, pp. 2294 – 2298.

[18] P. Stoica and J. Li, "Lecture notes - source localization from range-difference measurements," *IEEE Signal Process. Mag.*, vol. 23, no. 6, pp. 63–66, Nov. 2006.

[19] Y. Wang and G. Leus, "Reference-free time-based localization for an asynchronous target," *EURASIP J. Advances in Signal Processing*, 2012:19, Jan. 2012, doi:10.1186/1687-6180-2012-19.

[20] T. S. Rappaport, *Wireless Communications: Principles and Practice*, 2nd ed. Upper Saddle River, NJ: Prentice-Hall, Inc., 2002.

[21] R. Roy and T. Kailath, "ESPRIT-estimation of signal parameters via rotational invariance techniques," *IEEE Trans. Acoust., Speech, Signal Process.*, vol. 37, no. 7, pp. 984–995, Jul. 1989.

[22] T. K. Sarkar and O. Pereira, "Using the Matrix Pencil Method to Estimate the Parameters of a Sum of Complex Exponentials," *IEEE Antennas Propag. Mag.*, vol. 37, no. 1, pp. 48–55, Feb. 1995.

[23] B. Kusy, G. Balogh, J. Sallai, A. Lédeczi, and M. Maróti, "Intrack: high precision tracking of mobile sensor nodes," in *Proc. EWSN*, Delft, The Netherlands, Jul. 2007, pp. 51–66.

[24] I. Sarris and A. R. Nix, "Ricean K-factor measurements in a home and an office environment in the 60 GHz band," in *IST Mobile and Wireless Communications Summit*, Budapest, Hungary, Jul. 2007, pp. 1–5.